PHYSICAL REVIEW B VOLUME 56, NUMBER 8 15 AUGUST 1997-II

Electronic structures of $Sr_{14-x}Ca_xCu_{24}O_{41}$

Masao Arai
National Institute for Research in Inorganic Materials, Tsukuba, Ibaraki 305, Japan

Hirokazu Tsunetsugu
Institute of Applied Physics, University of Tsukuba, Tsukuba, Ibaraki 305, Japan

(Received 2 May 1997)

The electronic structures of $Sr_{14-x}Ca_xCu_{24}O_{41}$ are calculated within the local-density approximation. Around the Fermi energy there exist quasi-one-dimensional bands originated from the ladder and chain layers. The nearest-neighbor interladder hoppings are estimated to be 5–20 % of the intraladder ones. Possible effects of Ca substitution on electronic structures and charge distribution are also discussed. [S0163-1829(97)50332-8]

The doped spin-ladder compound, $Sr_{14-x}Ca_xCu_{24}O_{41}$, has recently attracted wide attention as a possible new class of superconductor. Superconductivity was observed at $x=13.6$ under high pressure 3.5–4 GPa.[1] The insulating phase has a finite spin gap, and the superconductivity is expected to be driven by the spin-liquid ground state, as theoretically predicted in Ref. 2.

The superconductivity appears upon substituting isovalent Ca for Sr, in addition to applying high pressure, whereas the formal Cu valence stays constant, 2.25 for all x. Considering this compound contains chain layers as well as ladder layers, this indicates that the local charge distribution may change with Ca substitution and with pressure, and that superconductivity needs a special charge distribution. Various experiments[3,4] and model calculations[5,6] have shown that most of the holes exist on the chains for $Sr_{14}Cu_{24}O_{41}$ and that the Ca substitution transfers the holes to ladder layers. In the present paper, we study the electronic structures and charge distribution of $Sr_{14-x}Ca_xCu_{24}O_{41}$ within the local density approximation (LDA).[7]

The crystal structures of $Sr_{14}Cu_{24}O_{41}$ and related compounds were reported in Refs. 8–12. They are composed of two subsystems, $Sr_2Cu_2O_3$ (ladders and Sr) and CuO_2 (chains). The chemical formula determined by structure analysis[12] is $(Sr_2Cu_2O_3)(CuO_2)_y$ with $y=1.436$. Due to interactions between the two subsystems, atomic positions of each subsystem are modulated by the periodicity of the other. Their structures were analyzed by assuming a large unit cell with y approximated by a rational number,[8,9] or by the super space-group technique.[10,12] If y is chosen as $\frac{7}{5}$ or $\frac{10}{7}$, the chemical formula becomes $Sr_{10}Cu_{17}O_{29}$ and $Sr_{14}Cu_{24}O_{41}$, respectively.

We have calculated the electronic structures for $M_{10}Cu_{17}O_{29}$ and $M_{14}Cu_{24}O_{41}$ (M = Sr or Ca). As a starting point, the structure modulation is ignored for simplicity. Possible effects of the modulation will be briefly discussed later. The symmetry of $M_{10}Cu_{17}O_{29}$ is chosen as face-centered orthorhombic $F222$ following Ref. 8. The a axis is perpendicular to the ladders and chains inside layers, the b axis perpendicular to stacking layers, and the c axis parallel to the chains and ladders. The lattice parameters are listed in Table I. $c_1(c_2)$ is the fundamental period of the ladder (chain) part along the c axis.

Even with the rational approximation, the crystal structure of $M_{10}Cu_{17}O_{29}$ is still complicated and the unit cell contains 56 atoms. Such a complicated structure is challenging for the *ab initio* calculation. We used the linear-muffin-tin-orbital (LMTO) method[13] with the atomic-sphere approximation, since this is suitable for a large unit cell. In addition to 56 atomic spheres, 44 empty spheres are inserted around Sr and CuO_2 chains. The positions and size of the empty spheres are optimized by the method explained in Ref. 14. We have performed the self-consistent calculations with 63 k points in the irreducible Brillouin zone for $M_{10}Cu_{17}O_{29}$ and 21 k points for $M_{14}Cu_{24}O_{41}$.

First, we show the total and partial density of states (DOS) in Fig. 1. The Fermi energy is set at $E_F=0$. The calculated DOS of $Sr_{10}Cu_{17}O_{29}$ and $Sr_{14}Cu_{24}O_{41}$ are similar to each other. This indicates that the small unit cell is enough to investigate the qualitative features. These compounds are calculated as a metal, leading to finite DOS at E_F. To reproduce experimentally observed insulating behavior, it would be necessary to take into account electron correlations along with possible charge ordering. The states in the region −7–2 eV are mainly composed of the Cu d and O p orbitals. Both Cu and O partial DOS distribute broadly in this energy region, which indicates strong hybridization of these orbitals. The Sr s orbitals slightly hybridize with the Cu d and O p orbitals, while their main weights appear at higher energy.

The width of the valence band is consistent with the photoemission experiments.[15] The two broad peaks observed in the photoemission spectrum at binding energy 3 eV and 5.5 eV are actually seen in the present calculation. The former peak may be assigned to the peaks of the total DOS at

TABLE I. Lattice constants (Å) used for calculations.

	$Sr_{10}Cu_{17}O_{24}$	$Sr_{14}Cu_{24}O_{41}$	$Ca_{10}Cu_{17}O_{24}$	$Ca_{14}Cu_{24}O_{41}$
a	11.46	11.46	11.46	11.18
b	13.40	13.40	12.40	12.40
c	19.40	27.65	19.40	27.10
c_1	3.88	3.95	3.88	3.87
c_2	2.77	2.76	2.77	2.71

 © 1997 The American Physical Society

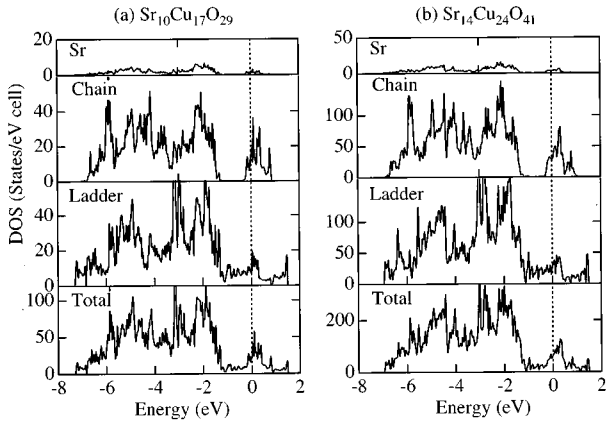

FIG. 1. The total and partial density of states of (a) $Sr_{10}Cu_{17}O_{29}$ and (b) $Sr_{14}Cu_{24}O_{41}$.

-2–-3 eV, and the latter peak around -5 eV. However, the position of Fermi energy is about 1 eV lower in the calculation. This may be because the Fermi energy is not correctly calculated for this metallic ground state.

The chain and ladder layers have different structures of partial DOS around E_F. The chain DOS forms a band with width of about 1 eV, separated from the main valence bands with an energy gap of 1 eV. On the other hand, the ladder DOS is smaller than the chain DOS and distributes in a wider energy region. The peaks at 0.1 eV and 1.5 eV in the ladder DOS are due to the edge singularity of two quasi-one-dimensional bands, as we shall explain later. The interlayer hybridization between ladders and chains seems to be small, since the peak positions of their partial DOS are not correlated.

We show the energy bands near E_F in Fig. 2. The bands are most dispersive along the symmetry line Γ-Z, which is parallel to chains and ladders, and then along Γ-X (perpendicular to chains and ladders in layers). The small dispersion perpendicular to layers (Γ-Y) indicates that the interlayer hoppings are weak. We identify the character of each state by the weights of various atomic orbitals. Most of states near E_F have their weights only on either chain layers or ladder layers. This verifies small interlayer hoppings, consistent with the dispersionless character along Γ-Y. We also find

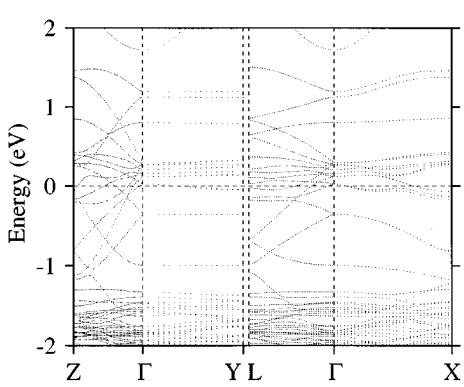

FIG. 2. The energy bands of $Sr_{10}Cu_{17}O_{29}$. Γ:(0,0,0), X: $(2\pi/a,0,0)$, Y:$(0,2\pi/b,0)$, Z:$(0,0,2\pi/c)$, and L:$(\pi/a,\pi/b,\pi/c)$.

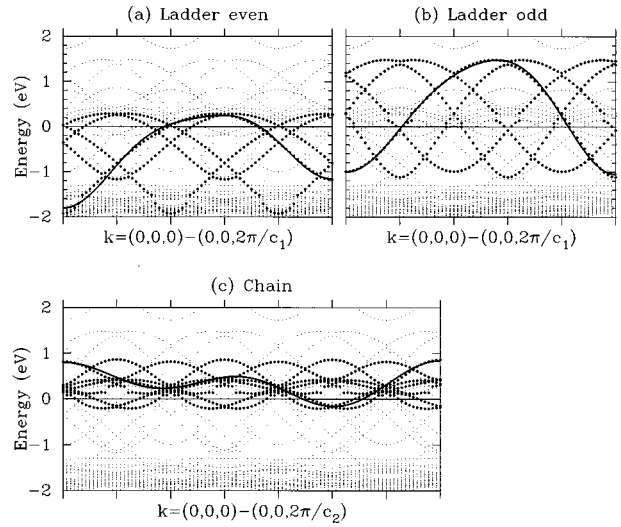

FIG. 3. The energy bands of $Sr_{10}Cu_{17}O_{29}$ in the extended Brillouin zone. Large dots represent (a) states on ladder layers with even mirror symmetry, (b) those on ladder layers with odd mirror symmetry, and (c) those on chain layers. Solid lines are numerical fit.

that the chain bands near E_F are mainly composed of the antibonding combination of Cu d_{xz} orbitals and O p_x and p_z orbitals, while the ladder bands are composed of Cu $d_{x^2-z^2}$ orbitals and O p_x and p_z orbitals.

We find that the calculated energy bands could be simply understood in the following way. To see that, we plot in Fig. 3 the chain and ladder bands separately in the *extended* Brillouin zone. The states with more than 15% of their weights on Cu $d_{x^2-z^2}$ orbitals in the ladders are shown with large dots in Figs. 3(a) and 3(b). The difference is that those in 3(a) and 3(b) have an even and odd parity, respectively, concerning the mirror symmetry perpendicular to the a axis. They both have the approximate periodicity of $2\pi/c=4\pi/c_1$, corresponding to the fundamental ladder period. Thus, it is reasonable to interpret that these bands are generated by the folding of an energy band between $\mathbf{k}=(0,0,0)$ and $(0,0,2\pi/c_1)$. The band can be fitted by the following tight-binding dispersion:

$$\epsilon_{\mathbf{k}}=\varepsilon_0-2t_1\cos(k_zc_1)-2t_2\cos(2k_zc_1)-[4t_1^{\perp}\cos(\tfrac{1}{2}k_zc_1)+4t_2^{\perp}\cos(\tfrac{3}{2}k_zc_1)]\cos(\tfrac{1}{2}k_xa), \quad (1)$$

where t_1 and t_2 are the nearest and second nearest-neighbor hoppings between rungs in the ladders, while $t_1^{\perp}$ and $t_2^{\perp}$ between adjacent ladders. The results are summarized in Table II and the fitting is also shown in Figs. 3(a) and 3(b). With the five parameters for each band, we can reproduce the overall features.

The interladder hoppings are 5–20 % of intraladder ones. These values suggest that the interladder hoppings may not be negligible in discussing the electronic structures and physical properties. Experimentally, the anisotropy of

TABLE II. Tight-binding parameters (eV) of the bands near E_F. The columns with ladder (+) and ladder (−) are for the ladder bands with even and odd mirror symmetry, respectively.

	$Sr_{10}Cu_{17}O_{24}$			$Ca_{10}Cu_{17}O_{24}$			$Sr_{14}Cu_{24}O_{41}$			$Ca_{14}Cu_{24}O_{41}$		
	ladder(+)	ladder(−)	chain	ladder(+)	ladder(−)	chain	ladder(+)	ladder(−)	chain	ladder(+)	ladder(−)	chain
ε_0	−0.48	0.35	0.34	−0.43	0.43	0.32	−0.31	0.46	0.33	−0.33	0.54	0.23
t_1	0.42	0.61	−0.09	0.44	0.61	−0.12	0.41	0.59	−0.09	0.44	0.62	−0.11
t_2	0.08	0.08	−0.15	0.10	0.08	−0.20	0.08	0.07	−0.17	0.10	0.07	−0.20
$t_1^{\perp}$	0.08	0.03	−0.03	0.08	0.04	−0.04	0.07	0.03	−0.03	0.08	0.07	−0.04
$t_2^{\perp}$	0.00	−0.04	0.03	0.00	−0.04	0.04	0.00	−0.04	0.03	0.00	−0.07	0.05

resistivity ρ_a/ρ_c is about 30 at temperature 100 K for $Sr_3Ca_{11}Cu_{24}O_{41}$,[16] larger than the present estimation, and it also has a large temperature dependence. Therefore it is natural to expect that the strong correlation effects such as hole pairing enhance the anisotropy, but we do not discuss it further in this paper. At high temperatures, the electron correlation may not be important and the present band anisotropy is consistent with the experiments.[16]

The chain bands near E_F also have a pseudo-one-dimensional character, while their dispersions are more complex, as shown in Fig. 2(c). Here large dots represent the states with more than 15% of their weights on Cu d_{xz} orbitals in the chain layers. We again fitted the dispersion by Eq. (1). The nearest-neighbor hoppings, t_1, along the chains are smaller than those for the ladder bands. This is because of the near 90° angle of Cu-O-Cu bonds.[6] The second nearest-neighbor hoppings, t_2, are largest and roughly twice the nearest-neighbor ones. The sign and relative ratio of these two, t_1 and t_2, are consistent with the semiquantitative estimation considering the spatial direction of atomic orbitals.

Next, we discuss the effects of Ca substitution which corresponds to positive chemical pressure. The unit cell volume decreases and the lattice constant b, i.e., the distance of subsequent layers, decreases most rapidly. We have calculated the electronic structure of fully substituted $Ca_{14}Cu_{24}O_{41}$ with the lattice constants extrapolated from the available experimental data.[1] The internal atomic positions are fixed to the same values with $Sr_{14}Cu_{24}O_{41}$. The total and partial DOS have similar features to those of $Sr_{14}Cu_{24}O_{41}$. The main change is a slight increase of the hybridization between Cu d orbitals and O p orbitals. The enhancement of the hybridization is actually found as the wider total bandwidth and the larger tight-binding hopping integrals shown in Table II. The increase is caused by the decrease of the atomic distance.

Let us now examine the hole distribution on the ladder and chain layers, which is important to investigate the origin of superconductivity under high pressure. We use the occupation ratio of the chain bands near E_F as a measure of the hole concentration. The bands are composed of the antibonding combination of Cu d_{xz} and O p_x and p_z orbitals. Setting the O valence to −2, we determine that the valence of chain Cu would be +1 if these bands are fully occupied, and +3 if completely empty. This is exact if the interlayer hybridization were absent and is expected to hold qualitatively in the present case, too.

With this assumption, we have calculated the chain Cu valence as $P_c = 3 - 2p$, where p is the occupation ratio of the chain DOS to the whole number of states in this energy region. The valence of Cu on the ladder layers, $P_{/\!/}$, is determined from the formal Cu valence $P_{\rm av}$ as $P_{/\!/} n_{/\!/} + P_c n_c = P_{\rm av}(n_{/\!/} + n_c)$ where $n_{/\!/}$ (n_c) is the number of Cu atoms on the ladder (chain) layers. The results are summarized in Table III. It is noticeable that the calculated Cu valence on the ladder layers is close to 2 while that on the chain layers shows a large deviation from 2. It means that most of the holes are on the chain layers. The Cu valence on the chain layers slightly decreases with the Ca substitution, indicating possible hole transfer from the chains to the ladders. However, the difference 0.02–0.05 is smaller than the proposed value, 0.18 for $x = 0 \rightarrow 11$, from optical measurement.[3]

So far, we have ignored structure modulations and possible change of internal atomic positions upon Ca substitution. Since the largest effect on charge distribution is via Madelung potential, the detailed crystal structure is important to take into account. We have evaluated the effect of atomic displacements using the crystal structures where Sr atoms are uniformly shifted in the b axis direction. If the shift is toward the chain layers, the potential for holes in the chain layers increases and the holes would move to the ladder layers.[6] Our calculations show that the ladder Cu valence changes about 0.06 for $b/100 = 0.13$ Å shift of Sr atoms.

Another important structure modulation is displacements of O atoms in the chain layers toward the apical positions of Cu atoms in the ladder layers.[17] Since O atoms in the chain layers approach positively charged Sr and Cu, the potential for holes on the chain layers increases and the holes would transfer to the ladder layers. We have performed the calculation for $Sr_{10}Cu_{17}O_{29}$ with the modulated structure reported in Ref. 8, with the lattice constants fixed. The ladder Cu valence increases to 1.98, compared to 1.93 for the unmodulated structure. These results indicate the importance of structure modulation to the hole doping in the ladders.

In summary, we have studied the electronic structures of $Sr_{14-x}Ca_xCu_{24}O_{41}$ within the local-density approximation. The total density of states is compared with photoemission experiments with fairly good agreement. The energy bands near Fermi energy are from the ladder and chain layers. They have a pseudo-one-dimensional character and the interladder

TABLE III. Estimated Cu valence.

	$Sr_{10}Cu_{17}O_{24}$	$Sr_{14}Cu_{24}O_{41}$	$Ca_{10}Cu_{17}O_{24}$	$Ca_{14}Cu_{24}O_{41}$
average	2.235	2.25	2.235	2.25
chain	2.67	2.64	2.62	2.62
ladder	1.93	1.97	1.97	1.99

hoppings are 5–20 % of the intraladder ones. The holes are mainly on the chains at $x=0$. The change of the lattice constant is not enough to transfer the holes to the ladders. Detailed atomic displacements have important effects on the hole distribution.

We would like to thank to O. K. Andersen and O. Jepsen for providing us the TB-LMTO-46 program. Part of the numerical calculations were performed on the NEC SX-3/4R at the Computer Center at the Institute for Molecular Science in Okazaki, Japan.

[1] M. Uehara, T. Nagata, J. Akimitsu, H. Takahashi, N. Môri, and K. Kinoshita, J. Phys. Soc. Jpn. **65**, 2764 (1996).

[2] E. Dagotto, J. Riera, and D. Scalapino, Phys. Rev. B **45**, 5744 (1992); M. Sigrist, T. M. Rice, and F. C. Zhang, *ibid.* **49**, 12 058 (1994); H. Tsunetsugu, M. Troyer, and T. M. Rice, *ibid.* **51**, 16 456 (1995).

[3] T. Osafune, N. Motoyama, H. Eisaki, and S. Uchida, Phys. Rev. Lett. **78**, 1980 (1997).

[4] Y. Kitaoka (private communication).

[5] M. Kato, K. Shiota, and Y. Koike, Physica C **258**, 284 (1996).

[6] Y. Mizuno, T. Tohyama, and S. Maekawa J. Phys. Soc. Jpn. **66** 937 (1997).

[7] For a review, see R. O. Jones and O. Gunnarsson, Rev. Mod. Phys. **61**, 689 (1989).

[8] K. Kato, E. Takayama-Muromachi, K. Kosuda, and Y. Uchida, Acta Crystallogr. Sect. C **44**, 1881 (1988).

[9] T. Siegrist, L. F. Schneemeyer, S. A. Sunshine, and J. V. Waszczak, Mater. Res. Bull. **23**, 1429 (1988).

[10] K. Kato, Acta Crystallogr. Sect. B **46**, 39 (1990).

[11] E. M. McCarron, III, M. A. Subramanian, J. C. Calabrese, and R. L. Harlow, Mater. Res. Bull. **23**, 1355 (1988).

[12] K. Ukei, T. Shishido, and T. Fukuda, Acta Crystallogr. Sect. B **50**, 42 (1994).

[13] O. K. Andersen, Phys. Rev. B **12**, 3060 (1975).

[14] O. Jepsen and O. K. Andersen, Z. Phys. B **97**, 35 (1995).

[15] T. Takahashi, T. Yokoya, A. Ashihara, O. Akaki, H. Fujisawa, A. Chainani, M. Uehara, T. Nagata, J. Akimitsu, and H. Tsunetsugu (unpublished).

[16] N. Motoyama, T. Osafume, T. Kakeshita, H. Eisaki, and S. Uchida, Phys. Rev. B **55**, R3386 (1997).

[17] T. Ohta, F. Izumi, M. Onoda, M. Isobe, E. Takayama-Muromachi, and A. W. Hewat (unpublished).